BIOCHEMISTRY
including biophysical chemistry & molecular biology
Article

Biochemistry **2010,** *49,* 2359–2367 2359
DOI: 10.1021/bi1000933

Naturally Occurring Variability in the Envelope Glycoprotein of HIV-1 and Development of Cell Entry Inhibitors†

Evan T. Brower, Arne Schön, and Ernesto Freire*

Department of Biology, The Johns Hopkins University, Baltimore, Maryland 21218

Received January 20, 2010; Revised Manuscript Received February 15, 2010

ABSTRACT: Naturally occurring genetic variability across HIV-1 subtypes causes amino acid polymorphisms in encoded HIV-1 proteins including the envelope glycoproteins associated with viral entry. The effects of amino acid polymorphisms on the mechanism of HIV-1 entry into cells, a process initiated by the binding of the viral envelope glycoprotein gp120 to the cellular CD4 receptor, are largely unknown. In this study, we demonstrate that amino acid polymorphisms affect the structural stability and domain cooperativity of gp120 and that those differences are reflected in the binding mechanism of the viral envelope glycoprotein to the cell surface receptor and coreceptor. Moreover, subtype differences also affect the binding behavior of experimental HIV cell entry inhibitors. While gp120-A has a slightly lower denaturation temperature than gp120-B, the most notable stability difference is that for gp120-B the van't Hoff to calorimetric enthalpy ratio ($\Delta H_{vH}/\Delta H$) is 0.95 whereas for gp120-A is 0.6, indicative of more cooperative domain/domain interactions in gp120-B, as this protein more closely approaches a two-state transition. Isothermal titration calorimetry demonstrates that CD4 and 17b (a surrogate antibody for the chemokine coreceptor) exhibit 7- and 3-fold weaker binding affinities for gp120-A. The binding of these proteins as well as that of the experimental entry inhibitor NBD-556 induces smaller conformational changes in gp120-A as evidenced by significantly smaller binding enthalpies and binding entropies. Together, these results describe the effects of gp120 polymorphisms on binding to host cell receptors and emphasize that guidelines for developing future entry inhibitors must recognize and deal with genomic differences between HIV strains.

The human immunodeficiency virus (HIV) pandemic remains a leading worldwide health concern, and continued development and optimization of antiretroviral therapies are necessary. Viral entry is an attractive point of intervention in the design of new antiretrovirals. HIV-1[1] entry into host cells is governed by interactions of the viral spike with target host cell receptors (*1*−*3*). The HIV-1 spike is composed of the gp120 exterior envelope glycoprotein and the gp41 transmembrane glycoprotein arranged into trimers on the virion surface. Entry is a sequence of events in which the HIV-1 gp120 glycoprotein first binds the CD4 receptor followed by the coreceptor, usually CCR5 or CXCR4, which elicits the gp41-mediated fusion of host cell and viral membranes (*3*, *4*). In the unliganded state, gp120 is composed of a structured core and large unstructured regions, and the coreceptor site is not well defined (*5*−*9*). Consequent to CD4 binding, gp120 experiences a massive structuring resulting in the structuring/activation of the coreceptor binding site (*5*, *7*, *9*, *10*).

The binding of CD4 to gp120 evokes unusually large changes in favorable enthalpy and unfavorable entropy, a thermodynamic signature that, together with a large negative heat capacity change, is reminiscent to that observed in protein folding (*5*, *7*−*10*). The so-called activation of the coreceptor site can be understood as a large scale folding of gp120, which includes the region corresponding to the coreceptor site. CD4 pays the energy penalty associated with structuring the gp120 coreceptor site, facilitating coreceptor binding and continuation of the viral entry process. The cooperative linkage between the CD4 and coreceptor binding sites in gp120 is usually analyzed using the monoclonal antibody 17b, a coreceptor surrogate used in biochemical studies that binds to the coreceptor site (*5*, *7*, *9*−*13*).

Until now, the cooperativity linkage between receptor and coreceptor binding sites in gp120 has only been studied within the context of the B subtype HIV-1 (*5*, *7*, *9*). However, only 10% of the global HIV infections are due to the B subtype prevalent in North America and Western Europe (*14*). Of the 33 million people currently infected with HIV-1, 67% or 22 million are in sub-Saharan Africa where the A and C subtypes account for the vast majority of infections (*14*). Due to the high mutation rate of the virus, the genetic variability within and between subtypes ranges from 15% to 20% and 25% to 30%, respectively (*15*), resulting in amino acid polymorphisms in encoded HIV-1 proteins, including the envelope glycoproteins. The significant role that polymorphisms play in the biochemical properties of HIV-1 proteins and inhibitor binding is not without precedent. This laboratory has previously demonstrated that HIV-1 protease polymorphisms result in A and C subtype proteases possessing higher structural stability than B subtype protease (*16*, *17*). In addition, polymorphisms present in HIV-1 protease from non-B subtype viruses modulate protease inhibitor potency and drug resistance (*17*−*19*). Considering that current antiretroviral therapy

†Supported by grants from the National Institutes of Health (GM 56550) and the National Science Foundation (MCB0131241).

*To whom correspondence should be addressed. Phone: (410) 516-7743. Fax: (410) 516-6469. E-mail: ef@jhu.edu.

[1]Abbreviations: HIV-1, human immunodeficiency virus type 1; gp120-A, gp120 from the A subtype 92UG031 HIV-1 isolate; gp120-B, gp120 from the B subtype YU2 HIV-1 isolate; DSC, differential scanning calorimetry; ITC, isothermal titration calorimetry; sCD4, soluble form of the human CD4 receptor; mAb, monoclonal antibody; SDS−PAGE, sodium dodecyl sulfate−polyacrylamide electrophoresis; DMSO, dimethyl sulfoxide.

Published on Web 02/19/2010

has been designed and tested with respect to targets from the less prevalent B subtype (*20*), a major issue is whether or not naturally occurring polymorphisms would affect the potency of antiretroviral therapies against different subtypes. A thermodynamic analysis of the effect of polymorphisms on the structural stability and cooperative linkage between binding sites in gp120 and their effects on experimental inhibitors is crucial for the development of broad spectrum viral entry inhibitors that are effective against all subtypes.

In this study, microcalorimetric techniques were used to compare stability and cooperative interactions in gp120 from clinical isolates of A and B subtype HIV-1 (henceforth referred to as gp120-A and gp120-B, respectively) and assess the impact of polymorphisms on its interactions with host cell receptors. Interestingly, the experimental entry inhibitor NBD-556 binds to gp120-A with a vastly different thermodynamic signature than to gp120-B. While NDB-556 was shown to act as a CD4 mimetic by structuring gp120-B upon binding (*9*), this effect is largely absent upon binding gp120-A, indicating polymorphisms between gp120-A and gp120-B may alter the mode of action of cell entry inhibitors. Taken together, these results indicate that gp120 polymorphisms must be taken into account in the development of entry inhibitors.

MATERIALS AND METHODS

Plasmids Expressing HIV-1 gp120 Envelope Glycoproteins. Throughout this paper, full-length gp120 from the B subtype YU2 HIV-1 isolate (GenBank accession no. M93258) and the A subtype 92UG031 HIV-1 isolate (GenBank accession no. L34667) are referred to as gp120-B and gp120-A, respectively. A pcDNA3.1/Zeo(−) expression vector (Invitrogen, Carlsbad, CA) containing the codon-optimized gene for gp120-B, with an N-terminal CD5 leader sequence and C-terminal $(His)_6$ tag, was kindly provided by J. Sodroski (Dana-Farber Cancer Institute, Harvard Medical School, Boston, MA). The codon-optimized gene for gp120-A was synthesized and inserted into pUC57 vector by GenScript Corp. (Piscataway, NJ). The gp120-A gene was amplified from the pUC57 plasmid by PCR using the following primers containing *Bst*EII and *Hin*dIII restriction sites (underlined in the primers): 5′-AAAAAAGGTGACCGTGTACTACGGCGTGCCCGTGTGGAAGG-3′; 5′-AAAAAAAAGCTTTCATCAGTGGTGGTGGTGGTGGTGCTTCTCCC-3′.

The gp120-B gene was cut out of the pcDNA3.1/Zeo(−) vector by digesting the plasmid with *Bst*EII and *Hin*dIII restriction enzymes, and the PCR amplified gp120-A gene containing *Bst*EII and *Hin*dIII restriction sites was also digested with these enzymes and ligated into the digested plasmid. The resulting pcDNA3.1/Zeo(−) expression vector contained the gp120-A gene with an N-terminal CD5 leader sequence and C-terminal $(His)_6$ tag. For the purpose of plasmid maintenance and amplification, the gp120-A and gp120-B expression constructs were transformed into *Escherichia coli* DH10B and stored as 15% glycerol stocks at −80 °C. DNA sequencing confirmed the sequences of the pcDNA3.1/Zeo(−) expression constructs containing either the gp120-A or gp120-B gene. The gp120-A and gp120-B amino acid residue numbering is based upon the prototypic envelope glycoproteins from the HIV-1 reference strain HXBc2 (*21*).

Expression of gp120-A and gp120-B. The pcDNA3.1/Zeo(−) expression constructs harboring the gp120-A or gp120-B genes were purified using the HiSpeed plasmid maxi kit from Qiagen (Germantown, MD) as directed by the manufacturer. The purified plasmids expressing codon-optimized gp120-A and gp120-B were transiently transfected into 293F suspension cells using the 293fectin reagent (Invitrogen) according to the manufacturer's protocol. The 293F cells were cultured at 37 °C in a humidified atmosphere with 8% CO_2 on an orbital shaking platform rotating at 115 rpm. The supernatant containing gp120-A or gp120-B was harvested 5 days after transfection.

Preparation and Purification of Protein. Prior to purification, the 293F cell supernatant containing gp120-A was filtered through a 0.45 μm membrane, concentrated approximately 4-fold using Centricon Plus-70 centrifugal filter devices (Millipore, Billerica, MA), and dialyzed into 20 mM Tris and 150 mM NaCl, pH 7.4. All column chromatography was completed on an AKTA FPLC system (Amersham Biosciences, Uppsala, Sweden). For purification of gp120-A, 75 mL of concentrated supernatant was applied to a 5 mL HisTrap HP column (GE Healthcare, Buckinghamshire, U.K.) that had been preequilibrated with 20 mM Tris and 150 mM NaCl, pH 7.4. gp120-A was eluted with a linear gradient of 20 mM Tris, 150 mM NaCl, and 300 mM imidazole, pH 7.4. Fractions containing gp120-A were pooled, concentrated, and loaded onto a HiLoad 16/60 Superdex 200 prep grade gel filtration column (GE Healthcare) previously equilibrated with PBS, pH 7.4 (Roche Diagnostics GmbH, Mannheim, Germany). The gel filtration column was developed with PBS, pH 7.4, and fractions containing monomeric gp120-A were pooled. For selection of properly folded and functional protein, approximately 20 mL of monomeric gp120-A was flowed over a 5 mL HiTrap NHS-activated HP column (GE Healthcare, Buckinghamshire, U.K.) conjugated with mAb F105 (Strategic Biosolutions, Newark, DE) that had been preequilibrated with PBS, pH 7.4, and gp120-A was eluted with 100 mM glycine and 150 mM NaCl, pH 2.4. Eluted fractions were immediately neutralized with 4 M Tris, pH 7.4, followed by dialysis into PBS, pH 7.4. gp120-A was concentrated to 4 μM and stored as 300 μL aliquots at −80 °C.

For purification of gp120-B, 293F cell supernatant containing gp120-B was filtered through a 0.45 μm membrane, concentrated approximately 6-fold using Centricon Plus-70 centrifugal filter devices (Millipore, Billerica, MA), and dialyzed into PBS, pH 7.4. About 20 mL of concentrated supernatant was purified over a 5 mL HiTrap NHS-activated HP column conjugated with mAb F105 exactly as described for gp120-A. gp120-B in PBS, pH 7.4, was concentrated to 4 μM and stored as 400 μL aliquots at −80 °C. gp120-A and gp120-B purity and approximate molecular masses of 90 kDa were confirmed by sodium dodecyl sulfate−polyacrylamide electrophoresis (SDS−PAGE). In order to determine the concentration of gp120-A and gp120-B solutions, absorbance at 280 nm was measured with an Agilent 8453 diode array spectrophotometer (Agilent, Santa Clara, CA). Extinction coefficients of 1.6 and 1.49 $(mg/mL)^{-1}$ cm^{-1} and molecular weights of 54933 and 53365 g/mol for gp120-A and gp120-B, respectively, were used to convert absorbance values to molar concentration. The extinction coefficients and molecular weights provided above correspond to deglycosylated gp120-A and gp120-B.

Soluble D1-D2-D3-D4 CD4 (sCD4) was generously provided by I. Chaiken (Drexel University College of Medicine, Philadelphia, PA). Monoclonal antibody 17b was made by Strategic Biosolutions. sCD4 and 17b were dialyzed into PBS, pH 7.4, and stored as 60 and 150 μM aliquots, respectively, at −80 °C.

Differential Scanning Calorimetry. The heat capacities of gp120-A and gp120-B were measured as a function of temperature

using a high-precision differential scanning VP-DSC microcalorimeter (Microcal Inc., Northampton, MA). Protein samples and reference solutions were extensively degassed and carefully loaded to prevent bubble formation in the calorimetric cells during the experiments. Thermal denaturation scans were conducted from 10 to 80 °C at a scan rate of 1 °C/min. Freshly dialyzed gp120-A and gp120-B solutions in PBS, pH 7.4, were used in the scans, each at a concentration of 1 mg/mL. Data were analyzed by software developed in this laboratory.

Isothermal Titration Calorimetry. Isothermal titration calorimetric experiments were performed using high-precision VP-ITC and iTC_{200} calorimetric systems from MicroCal Inc. The volume of the calorimetric cell in the VP-ITC is 1.4 mL, whereas the volume of cell in the iTC_{200} is 200 μL. Titrations of gp120-A and gp120-B were completed using iTC_{200} and VP-ITC calorimeters, respectively. All titrations detailed in this paper were conducted by adding the titrant in steps of 10 μL when using the VP-ITC or 1.4 μL when using the iTC_{200}. All solutions contained within the calorimetric cells and injector syringes were prepared in the same buffer, PBS, pH 7.4, with 2% dimethyl sulfoxide. NBD-556 was dissolved in 100% DMSO at a concentration of 10 mM. In titrations involving NBD-556, the syringe solution was prepared by dissolving the stock solution of NBD-556 and additional DMSO in PBS for a final DMSO concentration of 2%. Unless otherwise noted, experiments were conducted at a constant 25 °C. For the direct determination of the binding of sCD4 and 17b to gp120-A, the calorimetric cell containing 4 μM gp120-A was titrated with sCD4 or 17b each at a concentration of 40 μM. Direct binding of sCD4 and 17b to gp120-B was analyzed by titrating 2 μM gp120-B with sCD4 or 17b at a concentration of 30 or 20 μM, respectively. The binding of sCD4 to gp120-A and gp120-B was studied at different temperatures in the range of 15−37 °C. The direct binding of NBD-556 (generously supplied by A. Smith, III, University of Pennsylvania, Philadelphia, PA) to gp120-A was measured in experiments in which 4 μM gp120-A in the calorimetric cell was titrated with a solution of NBD-556 at a concentration of 150 μM. The binding of NDB-556 to gp120-A was analyzed across a temperature range of 10−25 °C.

To measure the effect of CD4 on the binding of 17b to gp120-A, a titration of gp120-A with sCD4 was followed immediately by a titration with 17b at a concentration of 30 μM. To measure the effect of CD4 on the binding of 17b to gp120-B, gp120-B prebound to sCD4 was titrated with 17b at a concentration of 20 μM. To analyze the effect of 17b on the binding of CD4 to gp120-A, gp120-A prebound to 17b was titrated with sCD4 at a concentration of 30 μM. To assess the effect of 17b on the binding of CD4 to gp120-B, gp120-B prebound to 17b was titrated with sCD4 at a concentration of 20 μM. All solutions were thoroughly degassed to avoid bubble formation in the calorimetric cell during stirring. The heat evolved upon each injection of ligand was obtained from the integral of the calorimetric signal. The heat associated with binding of a ligand to the protein in the cell was obtained by subtracting the heat of dilution from the heat of reaction. Heats of dilution due to any mismatch between the syringe and cell solutions were negligible in all experiments. The individual heats were plotted as a function of the molar ratio, and nonlinear regression of the data provided the enthalpy change (ΔH) and the association constant ($K_a = 1/K_d$). Because of the low affinity, the stoichiometry was fixed to a value corresponding to the percent active gp120-A (determined by titrating gp120-A with sCD4) for the binding of NBD-556 to gp120-A.

RESULTS AND DISCUSSION

Naturally Occurring Polymorphisms in gp120-A and gp120-B. Figure 1 illustrates the location of naturally occurring polymorphisms in gp120-A and gp120-B. The CD4 and coreceptor binding sites are highly conserved between the subtypes with most gp120 polymorphisms located away from these sites in the outer domain. In particular, helix α2 as well as the variable loops (V1−V5) carries a significant number of polymorphisms. In helix α2 9 out of 13 amino acids are different between the subtypes. Five of the nine polymorphisms, at positions 337 (Gln in gp120-B and Glu in gp120-A), 339 (Glu in gp120-B and Asn in gp120-A), 340 (Asn in gp120-B and Lys in gp120-A), 343 (Glu in gp120-B and Thr in gp120-A), and 347 (Ile in gp120-B and Lys in gp120-A) involve gain or loss of charged side chains, changes that may affect interactions between the outer domain and the rest of gp120. In the CD4 binding pocket, polymorphisms occur at positions 429 (Glu in gp120-B and Arg in gp120-A) and 474 (Asp in gp120-B and Asn in gp120-A). Three polymorphisms are present in the 17b binding site at positions 200 (Val in gp120-B and Ala in gp120-A), 419 (Arg in gp120-B and Lys in gp120-A), and 432 (Lys in gp120-B and Gln in gp120-A). Polymorphisms at positions 200 and 432, in addition to those at the CD4 binding pocket, are potentially significant because they are located in the bridging sheet. Variations in this region, which links the receptor and coreceptor binding sites (*12*), may affect the CD4-induced allosteric cascade that activates the coreceptor site. The location of the polymorphisms suggests that gp120-A and gp120-B may exhibit different structural stabilities and 17b binding energetics. Also, polymorphisms at positions 429 and 474, located directly at the entrance of the CD4 binding cavity, may directly influence the binding of CD4 inhibitors.

Structural Stability of gp120-A and gp120-B. The structural stability of full-length, fully glycosylated monomeric gp120 from the A subtype 92UG031 HIV-1 isolate (gp120-A) and the B subtype YU2 HIV-1 isolate (gp120-B) was assessed by differential scanning calorimetry (DSC), and the results are shown in Figure 2 and summarized in Table 1. Repeated scans of the same samples (not shown) indicate that the transition was ~85% reversible for both subtypes. The thermal unfolding transition for gp120-B shown in Figure 2 is centered at 61.1 °C. The enthalpy change for the folding/unfolding is 117 kcal/mol at the denaturation temperature, and the heat capacity change is 3.5 kcal K^{-1} mol^{-1}. The unfolding of gp120-A, shown in Figure 2, is centered at 58.4 °C and associated with an enthalpy change of 126 kcal/mol. The heat capacity change for both proteins is within error. The most notable difference between the gp120-B and gp120-A unfolding transition is that for gp120-B the van't Hoff to calorimetric enthalpy ratio ($\Delta H_{vH}/\Delta H$) is 0.95 whereas for gp120-A it is 0.6. This observation indicates that domain/domain interactions are more highly cooperative in gp120-B as this protein more closely approaches a two-state denaturation transition. The DSC results for gp120-B described here are similar to those reported previously (*7*), except that the deglycosylated molecular weight of gp120-B was used to normalize the data from the experiments presented here. When the thermodynamic data are used to calculate the Gibbs energy of stability of the two proteins at 37 °C, values of 5.7 and 5.3 kcal/mol, for gp120-A and gp120-B, respectively, are obtained, indicating that both proteins have similar stabilities at physiological temperature.

Both gp120-A and gp120-B denature at a temperature very similar to the median denaturation temperature of globular

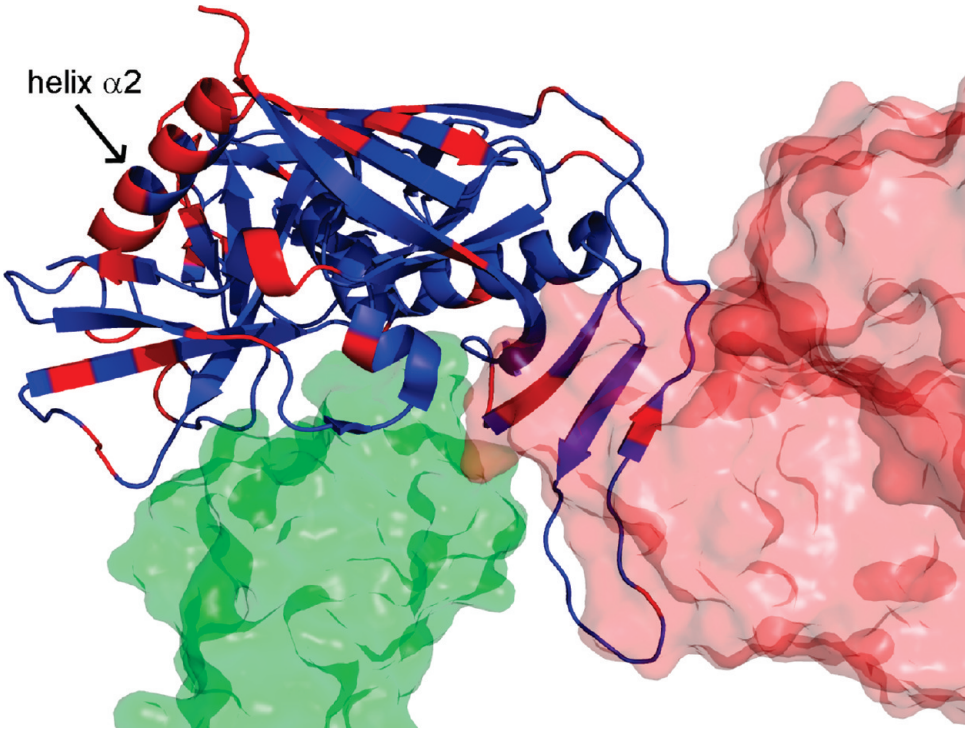

FIGURE 1: Naturally occurring amino acid polymorphisms between gp120 from the B subtype YU2 HIV-1 isolate and the A subtype 92UG031 HIV-1 isolate are shown in red on the structure of core gp120 shown in blue. CD4 and 17b are rendered as transparent green and red surfaces, respectively. The vast majority of the polymorphisms are located away from the highly conserved CD4 and coreceptor binding sites. In particular, helix α2 contains many polymorphisms (9 out of 13 residues). The structure corresponds to that of the gp120/CD4/17b ternary complex in PDB entry 1GC1 (*12*).

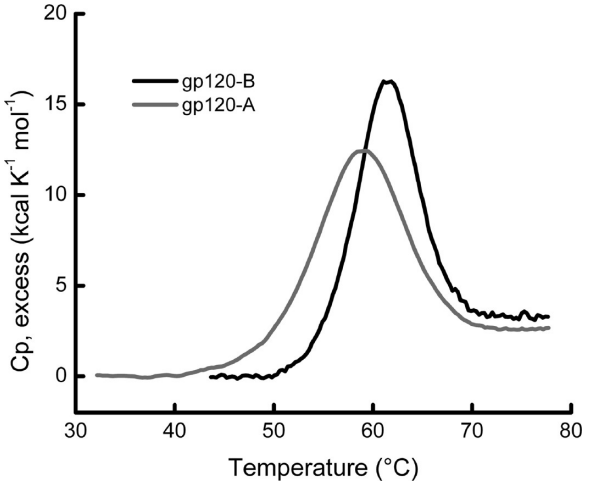

FIGURE 2: The temperature dependence of the heat capacity function of full-length, fully glycosylated gp120-A and gp120-B was measured using differential scanning calorimetry. gp120-A and gp120-B at a concentration of 1 mg/mL were used in the experiments.

proteins (*22*). When the thermodynamic parameters are normalized per gram of protein, it becomes apparent that the enthalpy changes for the folding/unfolding transitions of both glycoproteins at 60 °C are significantly smaller than the mean value observed for globular proteins. Specifically, the enthalpy changes at 60 °C for gp120-A and gp120-B (2.4 and 2.1 cal/g, respectively) are less than half of what is expected for the average globular protein at the same temperature. For example, at 60 °C the average globular protein exhibits an enthalpy change of 6.6 ± 1.7 cal/g (*22*). The mean heat capacity change for globular proteins is 0.12 ± 0.03 cal K^{-1} g^{-1} (*22*), significantly larger than

Table 1: Structural Stability of gp120-A and gp120-B[a]

protein	T_m (°C)	ΔH (kcal/mol)	ΔC_p (kcal/(K mol))
gp120-A	58.4 ± 0.1	126 ± 1.5	3.5 ± 0.7
gp120-B	61.1 ± 0.1	117 ± 2.0	3.5 ± 0.4

[a]Differential scanning calorimetry experiments were performed in PBS (pH 7.4) using gp120-A and gp120-B each at a concentration of 1 mg/mL. Thermal denaturation scans were performed at 1 °C/min from 10 to 80 °C.

the value obtained for gp120-A and gp120-B of 0.07 cal K^{-1} g^{-1}. Smaller than expected enthalpy and heat capacity changes denote that the core of the protein does not involve the expected number of residues and that a significant number of unstructured and solvent-exposed residues are present in the native state of both proteins. The observed energetics of the native state of gp120-B led to our previous conclusion that gp120 is comprised of a structured core and largely unstructured regions (*7*). The DSC data for gp120-A presented in this study indicate that the native state of gp120-A can also be described in the same manner, albeit with a slightly lower domain cooperativity. Judging by the location of most polymorphisms, it can be hypothesized that the interactions of the outer domain with the protein core are somewhat weaker.

Isothermal Titration Calorimetry of the Binding of CD4 and 17b to gp120-A. The impact of the existing polymorphisms between gp120-A and gp120-B on the binding thermodynamics to host cell receptors was measured using isothermal titration calorimetry (ITC). Figure 3 shows a calorimetric titration of gp120-A with sCD4 at 25 °C. The results are summarized in Table 2. The binding of CD4 to unliganded gp120-A is characterized by an affinity (K_d) of 110 nM in a process associated with large favorable and unfavorable changes in enthalpy and

entropy of −31.3 kcal/mol and −73 cal K^{-1} mol^{-1}, respectively. The change in heat capacity upon binding of CD4 to gp120-A, calculated from the temperature dependence of the binding enthalpy, is −1200 ± 80 cal K^{-1} mol^{-1} (Figure 3, inset). 17b binds to unliganded gp120-A with an affinity of 17 nM in a process where a large favorable enthalpy change of −17.9 kcal/mol is also partially compensated by an unfavorable entropy change of −24 cal K^{-1} mol^{-1}.

To measure the effect of CD4 on the binding of 17b to gp120-A, gp120-A prebound to CD4 was titrated with 17b. Likewise, the effect of 17b on the binding of CD4 was measured by titrating gp120-A prebound to 17b with CD4. The binding of 17b to the gp120-A/CD4 complex is characterized by an affinity of 12 nM and favorable enthalpy and entropy changes of −8.3 kcal/mol and 8.4 cal K^{-1} mol^{-1}, respectively. The binding of CD4 to the gp120-A/17b complex is described by an affinity of 80 nM and favorable and unfavorable changes in enthalpy and entropy of −21.7 kcal/mol and −40 cal K^{-1} mol^{-1}. The entire thermodynamic cycle for gp120-A, CD4, and 17b is presented in Figure 4.

Isothermal Titration Calorimetry of the Binding of CD4 and 17b to gp120-B. Isothermal titration calorimetric experiments were also conducted to study the binding of gp120-B to sCD4 and 17b under similar experimental conditions (Table 3). Unliganded gp120-B binds to CD4 with an affinity of 14 nM in a binding mode characterized by large enthalpic and entropic contributions of −37.6 kcal/mol and −90 cal K^{-1} mol^{-1}, respectively. The change in heat capacity for the binding of gp120-B to CD4 is −1600 ± 80 cal K^{-1} mol^{-1}. Unliganded gp120-B binds to 17b with an affinity of 5 nM. Similar to the binding of CD4, the antibody elicits large favorable and unfavorable changes in enthalpy and entropy of −33.8 kcal/mol and −75 cal K^{-1} mol^{-1}, respectively.

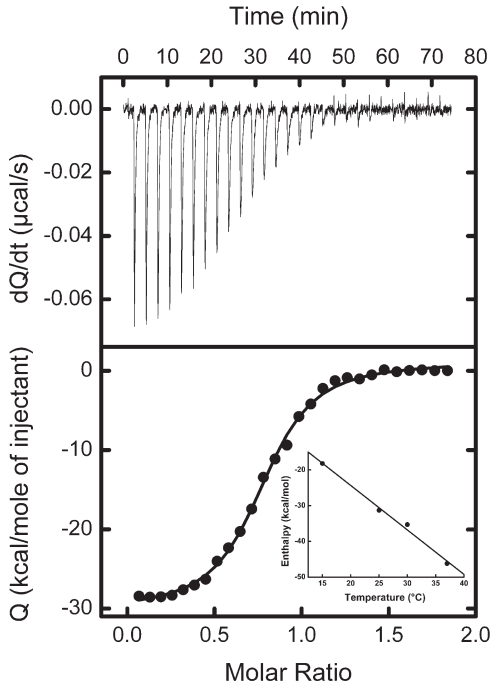

FIGURE 3: Microcalorimetric titration of gp120-A with sCD4 at 25 °C in PBS, pH 7.4, with 2% DMSO. gp120-A at a concentration of 4 μM in the calorimetric cell was titrated with 40 μM sCD4 contained in the injector syringe. The change in heat capacity was computed from the temperature dependence of the binding enthalpy (inset).

The effect of CD4 binding on the binding of gp120-B to 17b was characterized by titrating the gp120-B/CD4 complex with 17b. Likewise, gp120-B prebound to 17b was titrated with CD4 in order to understand the effect of 17b on the binding of gp120-B to CD4. The binding of 17b to the gp120-B/CD4 complex is characterized by an affinity of 2 nM and favorable enthalpy and entropy changes of −11.1 kcal/mol and 2 cal K^{-1} mol^{-1}, respectively. The binding of CD4 to the gp120-B/17b complex is characterized by an affinity of 6 nM and favorable and unfavorable changes in enthalpy and entropy of −14.9 kcal/mol and −12 cal K^{-1} mol^{-1}. The complete thermodynamic cycle for gp120-B, CD4, and 17b is presented in Figure 5. The binding data for gp120-B presented in this study are similar to previous results obtained in this laboratory (*5*, *7*, *9*). The large unfavorable entropy and large favorable enthalpy changes associated with the binding of gp120 to CD4 or 17b have been attributed to a large binding-induced structuring in gp120 that leads to the folding of the coreceptor site and consequently to a higher binding affinity (*5*, *7*−*9*, *13*).

Thermodynamic Signatures for gp120-A and gp120-B. Since the binding of gp120 to CD4 is an essential step in the entry of almost all clinical HIV-1 isolates (*3*), similar thermodynamic signatures could be expected for both gp120-A and gp120-B. In fact, the thermodynamic signatures of gp120-B and gp120-A binding to CD4 are similar (panels a and b of Figure 6, respectively) but not equal, indicating that the magnitude of the structuring effects is not the same in both cases. The affinity of gp120-A for sCD4 is about 8-fold weaker than that of gp120-B and is characterized by smaller enthalpy, entropy, and heat capacity changes (Tables 2 and 3). Similar effects are observed for the binding of 17b. A structure-based thermodynamic analysis of the CD4 binding data (*23*) indicates that binding to the receptor is consistent with the structuring of approximately 80 and 110 residues in gp120-A and gp120-B, respectively. In conjunction with the DSC experiments, the binding data suggest that unliganded gp120-A is more structured than unliganded gp120-B. The higher degree of intrinsic structure observed for gp120-A results in fewer conformational changes upon CD4 binding, indicating that some residues that become structured in

Table 2: Binding Thermodynamics of CD4, 17b, and NBD-556 to gp120-A[a]

component in ITC cell[b]	titrant	K_d (nM)	ΔG (kcal/mol)	ΔH (kcal/mol)	$-T\Delta S$ (kcal/mol)
gp120-A	sCD4	108 ± 9	−9.5 ± 0.04	−31.3 ± 1.1	21.8 ± 1.2
gp120-A	17b	17 ± 2	−10.6 ± 0.1	−17.9 ± 0.4	7.3 ± 0.2
gp120-A/CD4	17b	12 ± 4	−10.8 ± 0.3	−8.3 ± 0.8	−2.5 ± 0.3
gp120-A/17b	sCD4	80 ± 8	−9.7 ± 0.1	−21.7 ± 0.8	12.0 ± 0.6
gp120-A	NBD-556	5500 ± 700	−7.2 ± 0.1	−5.6 ± 0.2	−1.6 ± 0.1

[a]Isothermal titration calorimetry experiments were performed at 25 °C in PBS (pH 7.4) and 2% DMSO. [b]gp120-A prebound to sCD4 in the cell is depicted as gp120-A/CD4. gp120-A/17b denotes gp120-A prebound to 17b.

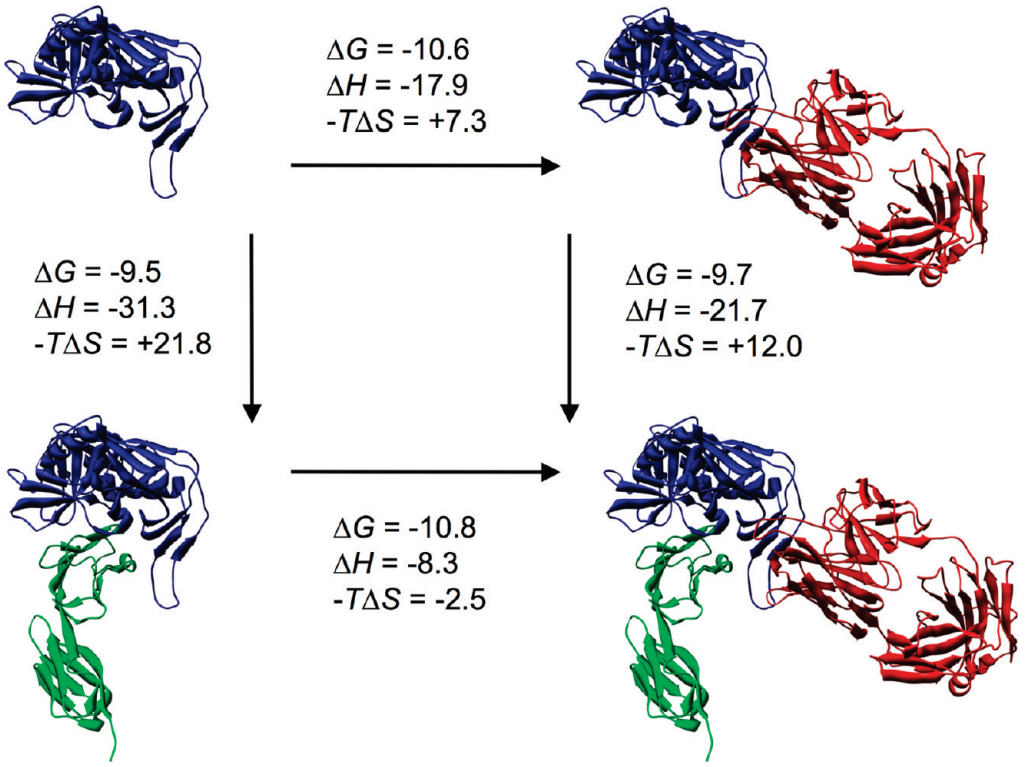

FIGURE 4: The thermodynamics of binding of CD4 (green) and 17b (red) to gp120-A (blue). All values were obtained from isothermal titration calorimetric experiments conducted at 25 °C, except values for ΔG and $-T\Delta S$ for the binding of 17b to gp120-A prebound to CD4 that were calculated by completing the thermodynamic cycle. The structures of gp120, sCD4, and 17b represent those found in PDB entry 1GC1 (*12*).

Table 3: Binding Thermodynamics of CD4, 17b, and NBD-556 to gp120-B[a]

component in ITC cell[b]	titrant	K_d (nM)	ΔG (kcal/mol)	ΔH (kcal/mol)	$-T\Delta S$ (kcal/mol)
gp120-B	sCD4	14 ± 2	−10.7 ± 0.1	−37.6 ± 1.0	26.9 ± 1.0
gp120-B	17b	5 ± 1	−11.3 ± 0.2	−33.8 ± 0.7	22.5 ± 0.6
gp120-B/CD4	17b	2 ± 1	−11.8 ± 0.4	−11.1 ± 0.3	−0.7 ± 0.04
gp120-B/17b	sCD4	6 ± 1	−11.2 ± 0.1	−14.9 ± 1.1	3.7 ± 0.3
gp120-B	NBD-556[c]	3700	−7.4	−24.5	17.1

[a]Isothermal titration calorimetry experiments were performed at 25 °C in PBS (pH 7.4) and 2% DMSO. [b]gp120-B prebound to sCD4 in the cell is depicted as gp120-B/CD4. gp120-B/17b denotes gp120-B prebound to 17b. [c]The energetics of NBD-556 binding to gp120-B were presented in a previous study (*9*).

gp120-B upon CD4 binding are already structured in gp120-A prior to receptor binding.

17b-induced structuring of gp120-B and gp120-A is also evident in the measured large enthalpic and entropic contributions to binding (Tables 2 and 3). Although the 17b epitope is highly conserved between the two proteins, three polymorphisms are present in the 17b binding site at positions 200 (Val in gp120-B and Ala in gp120-A), 419 (Arg in gp120-B and Lys in gp120-A), 431 (Gly in gp120-B and Glu in gp120-A), and 432 (Lys in gp120-B and Gln in gp120-A). 17b exhibits 3-fold weaker affinity for unliganded gp120-A. While the overall thermodynamic signatures are relatively similar, the magnitude of the enthalpy and entropy changes upon 17b binding to gp120-A is smaller than that for gp120-B. In particular, the entropic penalty is lower for 17b binding to gp120-A than to gp120-B.

Contrary to the large enthalpy and entropy changes observed when unliganded gp120-A or gp120-B is titrated with CD4 or 17b, the binding of 17b to either glycoprotein prebound to CD4 is characterized by significantly smaller thermodynamic quantities (Tables 2 and 3 and Figure 6e,f) (*5*−*7*, *9*, *10*, *13*) reminiscent of normal protein−protein interactions where only local conformational changes occur (*24*, *25*). CD4 increases the binding affinity of 17b for gp120-B (*5*−*7*, *9*, *10*, *13*), but the affinity enhancement effect is minimal for gp120-A and within experimental error.

The exact reasons by which subtype variability affects viral pathogenesis are still unknown. Nonetheless, several studies have shown that patients infected with A subtype HIV-1 progress to AIDS more slowly than those infected with C, D, or G subtype HIV-1 (*26*−*28*). Most likely, a combination of factors including polymorphisms in gp120 may contribute to the slower rate of disease progression observed for A subtype HIV-1.

Isothermal Titration Calorimetry of the Binding of NBD-556 to gp120-A and gp120-B. NBD-556 (structure shown in Figure 7b) and its analogues are experimental viral entry inhibitors (*9*, *13*, *29*). These low molecular weight compounds inhibit viral entry by competitively blocking binding of CD4 to gp120 (*9*, *13*, *29*). Specifically, these compounds target the conserved Phe 43 cavity in gp120 critical to receptor binding, preventing extension of Phe 43 of CD4 into this pocket (*13*). In cell-based entry assays, NDB-556 and analogues inhibit HIV-1

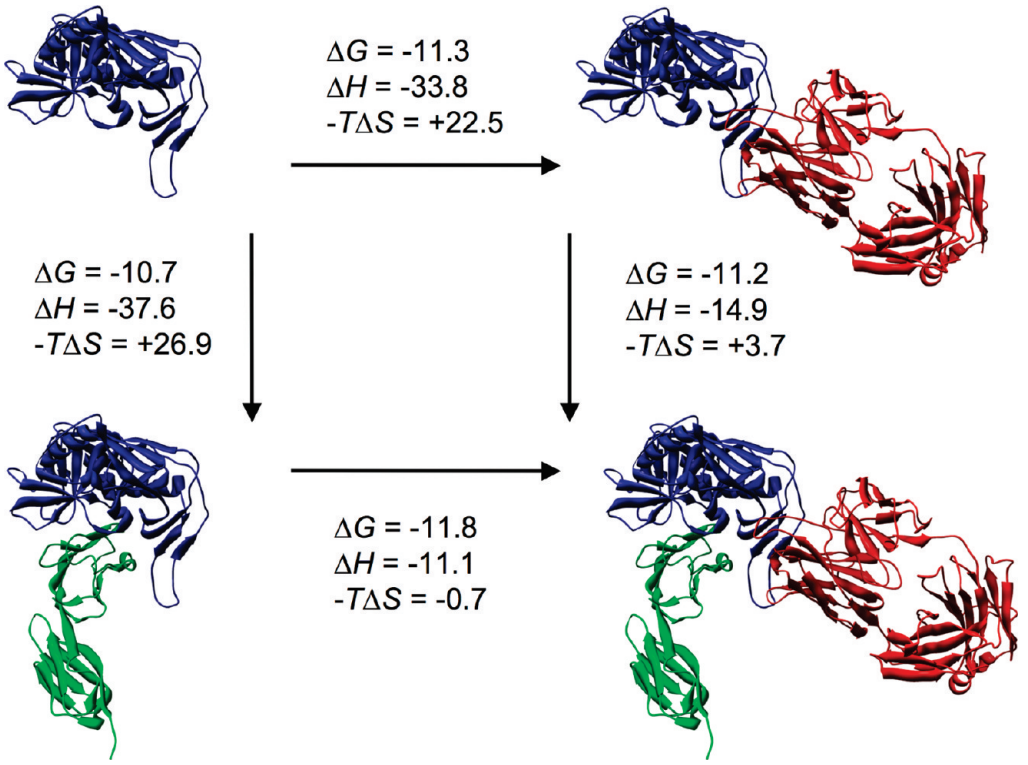

FIGURE 5: The thermodynamics of binding of CD4 (green) and 17b (red) to gp120-B (blue). All values were obtained from isothermal titration calorimetric experiments conducted at 25 °C, except values for ΔG and $-T\Delta S$ for the binding of 17b to gp120-B prebound to CD4 that were calculated by completing the thermodynamic cycle. The structures of gp120, sCD4, and 17b represent those found in PDB entry 1GC1 (*12*).

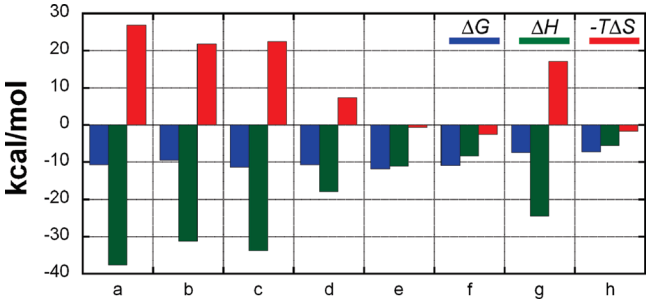

FIGURE 6: Thermodynamic signature for binding of (a) sCD4 to unliganded gp120-B, (b) sCD4 to unliganded gp120-A, (c) mAb 17b to unliganded gp120-B, (d) 17b to unliganded gp120-A, (e) 17b to gp120-B prebound to sCD4, (f) 17b to gp120-A prebound to sCD4, (g) NDB-556 to unliganded gp120-B (*9*), and (h) NBD-556 to unliganded gp120-A.

infection of cells expressing CD4 and CCR5 ($CD4^+CCR5^+$) (*13*). The inhibition of viral infectivity relates to the binding affinity of these compounds for gp120-B, with higher affinity compounds exhibiting more efficient entry inhibition (*13*). These compounds also act as true CD4 mimetics, in that they enhance HIV-1 infection of cells expressing CCR5 but not CD4 ($CD4^-CCR5^+$ cells) (*9*, *13*).

The binding thermodynamics of NBD-556 has only been measured against gp120-B (*9*). In order to assess the effect of gp120 polymorphisms on NBD-556 binding, ITC was used to measure the thermodynamics of NBD-556 binding to gp120-A. The binding of NBD-556 to unliganded gp120-A is characterized by an affinity of 5.5 μM in a process characterized by favorable changes in enthalpy and entropy of -5.6 kcal/mol and 5.4 cal K^{-1} mol^{-1}, respectively. The change in heat capacity for the binding of NDB-556 to gp120-A is near zero. As previously reported, NBD-556 binds gp120-B with a binding affinity of

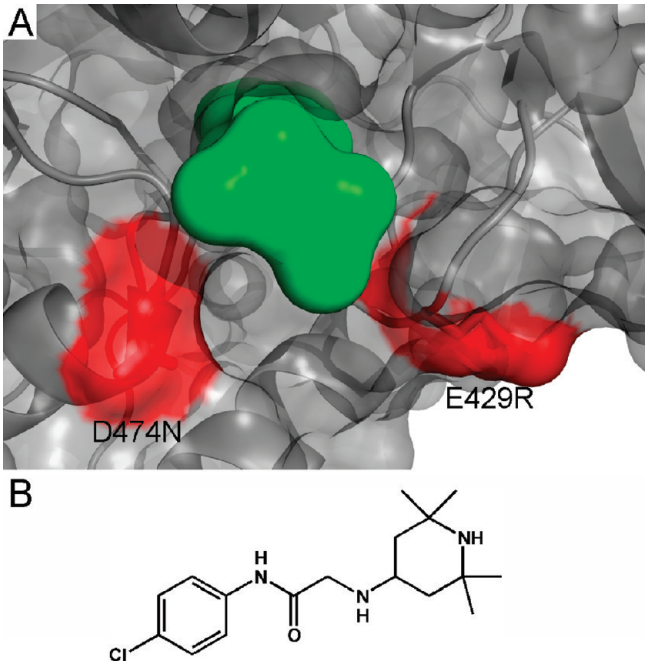

FIGURE 7: (a) The Phe 43 cavity of gp120 showing the van der Waals surface of NBD-556 in green. NDB-556 is shown docked into the structure of gp120-B (1g9n) (*13*). Amino acid polymorphisms within 5 Å of the inhibitor are shown in red. At position 429 the Glu present in gp120-B is replaced by Arg in gp120-A, and at position 474 the Asp present in gp120-B is substituted by Asn in gp120-A. (b) The structure of NBD-556.

3.7 μM and large favorable and unfavorable changes in enthalpy and entropy of -24.5 kcal/mol and -57.4 cal K^{-1} mol^{-1}, respectively, and a change in heat capacity of -1000 ± 50 cal K^{-1} mol^{-1} (*9*).

The thermodynamic signatures of NBD-556 binding to gp120-B and gp120-A are illustrated in panels g and h of Figure 6, respectively. The thermodynamic signature for the binding of NBD-556 to gp120-B resembles that of CD4 binding to this protein (large favorable enthalpy, large unfavorable entropy, large negative heat capacity change) (*9*). NBD-556 acts like a true CD4 mimetic, structuring approximately 67 residues upon binding gp120-B and enhancing coreceptor binding (*9*). The thermodynamic values obtained for the binding of NBD-556 to gp120-A are strikingly different. Although the binding affinities, and consequently the changes in Gibbs energy, are similar (−7.2 and −7.4 kcal/mol, respectively), the binding of NBD-556 to gp120-A is characterized by enthalpic and entropic binding changes considerably smaller in magnitude and a negligible change in heat capacity. In fact, the binding thermodynamics of NBD-556 to gp120-A resembles what is commonly observed for small molecules that bind without inducing a large structuring in their targets (*30*, *31*).

From a purely thermodynamic perspective, the overall Gibbs energy of binding, ΔG, can be separated into two terms:

$$\Delta G = \Delta G_{int} + \Delta G_{conf} \quad (1)$$

where ΔG_{int} and ΔG_{conf} are intrinsic and conformational components, respectively, of the overall binding energy. ΔG_{int} is equivalent to the binding energy that would be observed if gp120 were in the bound conformation prior to binding. ΔG_{conf} is equal to the energy associated with the conformational change upon binding and is an unfavorable term because gp120 cannot spontaneously complete the conformational change when no ligand is present. The overall Gibbs energies of binding of NBD-556 to gp120-A and gp120-B are very similar despite the larger structuring that takes place upon binding to gp120-B. Accordingly, it can be assumed that a larger unfavorable ΔG_{conf} is associated with binding to gp120-B. If this is the case, ΔG_{int} must be more favorable for the binding of NBD-556 to gp120-B than to gp120-A. If the strength of the interactions between NBD-556 and gp120-A were the same as those with gp120-B, the binding affinity of NBD-556 would have been significantly higher for gp120-A because the large, unfavorable entropic penalty observed when NBD-556 binds to gp120-B is significantly smaller for gp120-A.

NBD-556 binds deep into the Phe 43 cavity in gp120 as illustrated in Figure 7 (*13*). Figure 7 illustrates NDB-556 docked into the structure of gp120-B (*13*) and also shows the two gp120 polymorphisms located within 5 Å of NBD-556 at positions 429 (Glu in gp120-B and Arg in gp120-A) and 474 (Asp in gp120-B and Asn in gp120-A). Madani and co-workers (*13*) studied the effects of gp120-B mutations on the ability of NDB-556 and analogues to enhance infection of $CD4^{-}CCR5^{+}$ cells. These authors found that the E429K mutation in gp120-B eradicated the NBD-556-induced enhancement of infection (*13*). In gp120-B, Glu 429 forms a salt bridge with Lys 121 in the bridging sheet. Substitution of Glu 429 with a Lys or Arg residue would disrupt the salt bridge and potentially interfere with the ability of NBD-556 or similar compounds to structure and activate the gp120 coreceptor site. However, it must be noted that the extensive polymorphisms distal to the receptor and coreceptor sites may also play a role in the conformational cascade triggered by binding. Regardless of the location of polymorphisms, it is apparent that the development of wide spectrum viral entry inhibitors must address the issue of target polymorphisms and their effects on affinity and inhibitory activity.

CONCLUSIONS

The efficacy of antiretroviral therapies is always hampered by amino acid polymorphisms in the target molecules. These polymorphisms originate from genomic differences in clinical isolates, from variations between viral subtypes and once a therapy is established, as a result of mutations associated with drug resistance. The experience with HIV-1 protease inhibitors and reverse transcriptase inhibitors has shown that a low susceptibility to polymorphisms and mutations associated with drug resistance must be one of the most important characteristics of inhibitors (*16*−*19*, *32*−*37*). The studies presented in this report demonstrate that amino acid polymorphisms between gp120 from A and B subtype HIV-1 isolates affect the structural and binding properties of these proteins and may have a profound effect on their response to potential viral entry inhibitors. While NBD-556 acts a true CD4 mimetic upon binding gp120-B, inducing large scale conformational changes, the same compound has no analogous measurable effect on gp120-A, despite the fact that it exhibits similar binding affinity toward the two subtypes. Targeting allosteric proteins requires simultaneous consideration of both binding affinity and cooperative allosteric effects since they are not necessarily correlated. A successful viral entry inhibitor must exhibit high affinity against different subtypes and should not elicit unwanted allosteric effects. The results presented here emphasize that the development of future broad spectrum viral entry inhibitors requires explicit consideration of between and within subtype amino acid polymorphisms.

ACKNOWLEDGMENT

We thank Dr. Amos Smith, III (University of Pennsylvania), for providing NDB-556 used in these studies. We also thank Dr. Joseph Sodroski (Dana-Farber Cancer Institute, Harvard Medical School) for helpful discussions and Drs. Teresa Groesch and Sonia Yan Lam for help with protein purification.

REFERENCES

1. Chan, D. C., Fass, D., Berger, J. M., and Kim, P. S. (1997) Core structure of gp41 from the HIV envelope glycoprotein. *Cell 89*, 263–273.
2. Kowalski, M., Potz, J., Basiripour, L., Dorfman, T., Goh, W. C., Terwilliger, E., Dayton, A., Rosen, C., Haseltine, W., and Sodroski, J. (1987) Functional regions of the envelope glycoprotein of human immunodeficiency virus type 1. *Science 237*, 1351–1355.
3. Wyatt, R., and Sodroski, J. (1998) The HIV-1 envelope glycoproteins: fusogens, antigens, and immunogens. *Science 280*, 1884–1888.
4. Berger, E. A., Murphy, P. M., and Farber, J. M. (1999) Chemokine receptors as HIV-1 coreceptors: roles in viral entry, tropism, and disease. *Annu. Rev. Immunol. 17*, 657–700.
5. Brower, E. T., Schon, A., Klein, J. C., and Freire, E. (2009) Binding thermodynamics of the N-terminal peptide of the CCR5 coreceptor to HIV-1 envelope glycoprotein gp120. *Biochemistry 48*, 779–785.
6. Kwong, P. D., Doyle, M. L., Casper, D. J., Cicala, C., Leavitt, S. A., Majeed, S., Steenbeke, T. D., Venturi, M., Chaiken, I., Fung, M., Katinger, H., Parren, P. W., Robinson, J., Van Ryk, D., Wang, L., Burton, D. R., Freire, E., Wyatt, R., Sodroski, J., Hendrickson, W. A., and Arthos, J. (2002) HIV-1 evades antibody-mediated neutralization through conformational masking of receptor-binding sites. *Nature 420*, 678–682.
7. Leavitt, S. A., SchOn, A., Klein, J. C., Manjappara, U., Chaiken, I. M., and Freire, E. (2004) Interactions of HIV-1 proteins gp120 and Nef with cellular partners define a novel allosteric paradigm. *Curr. Protein Pept. Sci. 5*, 1–8.
8. Myszka, D. G., Sweet, R. W., Hensley, P., Brigham-Burke, M., Kwong, P. D., Hendrickson, W. A., Wyatt, R., Sodroski, J., and Doyle, M. L. (2000) Energetics of the HIV gp120-CD4 binding reaction. *Proc. Natl. Acad. Sci. U.S.A. 97*, 9026–9031.
9. Schön, A., Madani, N., Klein, J. C., Hubicki, A., Ng, D., Yang, X., Smith, A. B., 3rd, Sodroski, J., and Freire, E. (2006) Thermodynamics

of binding of a low-molecular-weight CD4 mimetic to HIV-1 gp120. *Biochemistry 45*, 10973–10980.
10. Schön, A., and Freire, E. (2007) Strategies for targeting HIV-1 envelope glycoproteins gp120 in the development of new antivirals. *Future HIV Ther. 1*, 223–229.
11. Kwong, P. D., Wyatt, R., Majeed, S., Robinson, J., Sweet, R. W., Sodroski, J., and Hendrickson, W. A. (2000) Structures of HIV-1 gp120 envelope glycoproteins from laboratory-adapted and primary isolates. *Structure 8*, 1329–1339.
12. Kwong, P. D., Wyatt, R., Robinson, J., Sweet, R. W., Sodroski, J., and Hendrickson, W. A. (1998) Structure of an HIV gp120 envelope glycoprotein in complex with the CD4 receptor and a neutralizing human antibody. *Nature 393*, 648–659.
13. Madani, N., Schon, A., Princiotto, A. M., Lalonde, J. M., Courter, J. R., Soeta, T., Ng, D., Wang, L., Brower, E. T., Xiang, S. H., Do Kwon, Y., Huang, C. C., Wyatt, R., Kwong, P. D., Freire, E., Smith, A. B., III, and Sodroski, J. (2008) Small-molecule CD4 mimics interact with a highly conserved pocket on HIV-1 gp120. *Structure 16*, 1689–1701.
14. UNAIDS (2008) 2008 Report on the global AIDS epidemic, *Geneva: UNAIDS* (www.unaids.org).
15. Korber, B., Gaschen, B., Yusim, K., Thakallapally, R., Kesmir, C., and Detours, V. (2001) Evolutionary and immunological implications of contemporary HIV-1 variation. *Br. Med. Bull. 58*, 19–42.
16. Velazquez-Campoy, A., Todd, M. J., Vega, S., and Freire, E. (2001) Catalytic efficiency and vitality of HIV-1 proteases from African viral subtypes. *Proc. Natl. Acad. Sci. U.S.A. 98*, 6062–6067.
17. Velazquez-Campoy, A., Vega, S., Fleming, E., Bacha, U., Sayed, Y., Dirr, H. W., and Freire, E. (2003) Protease inhibition in African subtypes of HIV-1. *AIDS Rev. 5*, 165–171.
18. Brower, E. T., Bacha, U. M., Kawasaki, Y., and Freire, E. (2008) Inhibition of HIV-2 protease by HIV-1 protease inhibitors in clinical use. *Chem. Biol. Drug Des. 71*, 298–305.
19. Velazquez-Campoy, A., Vega, S., and Freire, E. (2002) Amplification of the effects of drug resistance mutations by background polymorphisms in HIV-1 protease from African subtypes. *Biochemistry 41*, 8613–8619.
20. Perrin, L., Kaiser, L., and Yerly, S. (2003) Travel and the spread of HIV-1 genetic variants. *Lancet Infect. Dis. 3*, 22–27.
21. Korber, B., Foley, B., Kuiken, C., Pillai, S., and Sodroski, J. (1998) Numbering positions in HIV relative to HXBc2, Human retroviruses and AIDS 1998, Los Alamos National Laboratory, Los Alamos, NM.
22. Robertson, A. D., and Murphy, K. P. (1997) Protein structure and the energetics of protein stability. *Chem. Rev. 97*, 1251–1267.
23. Luque, I., and Freire, E. (1998) Structure-based prediction of binding affinities and molecular design of peptide ligands. *Methods Enzymol. 295*, 100–127.
24. Schwarz, F. P., Tello, D., Goldbaum, F. A., Mariuzza, R. A., and Poljak, R. J. (1995) Thermodynamics of antigen-antibody binding using specific anti-lysozyme antibodies. *Eur. J. Biochem. 228*, 388–394.
25. Sundberg, E. J., Urrutia, M., Braden, B. C., Isern, J., Tsuchiya, D., Fields, B. A., Malchiodi, E. L., Tormo, J., Schwarz, F. P., and Mariuzza, R. A. (2000) Estimation of the hydrophobic effect in an antigen-antibody protein-protein interface. *Biochemistry 39*, 15375–15387.
26. Kanki, P. J., Hamel, D. J., Sankale, J. L., Hsieh, C., Thior, I., Barin, F., Woodcock, S. A., Gueye-Ndiaye, A., Zhang, E., Montano, M., Siby, T., Marlink, R., I, N. D., Essex, M. E., and Mboup, S. (1999) Human immunodeficiency virus type 1 subtypes differ in disease progression. *J. Infect. Dis. 179*, 68–73.
27. Kiwanuka, N., Laeyendecker, O., Robb, M., Kigozi, G., Arroyo, M., McCutchan, F., Eller, L. A., Eller, M., Makumbi, F., Birx, D., Wabwire-Mangen, F., Serwadda, D., Sewankambo, N. K., Quinn, T. C., Wawer, M., and Gray, R. (2008) Effect of human immunodeficiency virus type 1 (HIV-1) subtype on disease progression in persons from Rakai, Uganda, with incident HIV-1 infection. *J. Infect. Dis. 197*, 707–713.
28. Kuritzkes, D. R. (2008) HIV-1 subtype as a determinant of disease progression. *J. Infect. Dis. 197*, 638–639.
29. Zhao, Q., Ma, L., Jiang, S., Lu, H., Liu, S., He, Y., Strick, N., Neamati, N., and Debnath, A. K. (2005) Identification of N-phenyl-N′-(2,2,6,6-tetramethyl-piperidin-4-yl)-oxalamides as a new class of HIV-1 entry inhibitors that prevent gp120 binding to CD4. *Virology 339*, 213–225.
30. Mobley, D. L., and Dill, K. A. (2009) Binding of small-molecule ligands to proteins: "what you see" is not always "what you get. *Structure 17*, 489–498.
31. Ohtaka, H., and Freire, E. (2005) Adaptive inhibitors of the HIV-1 protease. *Prog. Biophys. Mol. Biol. 88*, 193–208.
32. Alexander, C. S., Montessori, V., Wynhoven, B., Dong, W., Chan, K., O′Shaughnessy, M. V., Mo, T., Piaseczny, M., Montaner, J. S. G., and Harrigan, P. R. (2002) Prevalence and response to antiretroviral therapy of non-B subtypes of HIV in antiretroviral-naive individuals in British Columbia. *Antivir. Ther. 7*, 31–35.
33. Becker-Pergola, G., Kataaha, P., Johnston-Dow, L., Fung, S., Jackson, J. B., and Eshleman, S. H. (2000) Analysis of HIV type 1 protease and reverse transcriptase in antiretroviral drug-naive Ugandan adults. *AIDS Res. Hum. Retroviruses 16*, 807–813.
34. Bocket, L., Cheret, A., Deuffic-Burban, S., Choisy, P., Gerard, Y., de la Tribonniere, X., Viget, N., Ajana, F., Goffard, A., Barin, F., Mouton, Y., and Yazdanpanah, Y. (2005) Impact of human immunodeficiency virus type 1 subtype on first-line antiretroviral therapy effectiveness. *Antivir. Ther. 10*, 247–254.
35. Frater, A. J., Dunn, D. T., Beardall, A. J., Ariyoshi, K., Clarke, J. R., McClure, M. O., and Weber, J. N. (2002) Comparative response of African HIV-1-infected individuals to highly active antiretroviral therapy. *AIDS 16*, 1139–1146.
36. Pillay, D., Walker, A. S., Gibb, D. M., de Rossi, A., Kaye, S., Ait-Khaled, M., Munoz-Fernandez, M., and Babiker, A. (2002) Impact of human immunodeficiency virus type 1 subtypes on virologic response and emergence of drug resistance among children in the Pediatric European Network for Treatment of AIDS (PENTA) 5 trial. *J. Infect. Dis. 186*, 617–625.
37. van de Vijver, D. A., Wensing, A. M., Angarano, G., Asjo, B., Balotta, C., Boeri, E., Camacho, R., Chaix, M. L., Costagliola, D., De Luca, A., Derdelinckx, I., Grossman, Z., Hamouda, O., Hatzakis, A., Hemmer, R., Hoepelman, A., Horban, A., Korn, K., Kucherer, C., Leitner, T., Loveday, C., MacRae, E., Maljkovic, I., de Mendoza, C., Meyer, L., Nielsen, C., Op de Coul, E. L., Ormaasen, V., Paraskevis, D., Perrin, L., Puchhammer-Stockl, E., Ruiz, L., Salminen, M., Schmit, J. C., Schneider, F., Schuurman, R., Soriano, V., Stanczak, G., Stanojevic, M., Vandamme, A. M., Van Laethem, K., Violin, M., Wilbe, K., Yerly, S., Zazzi, M., and Boucher, C. A. (2006) The calculated genetic barrier for antiretroviral drug resistance substitutions is largely similar for different HIV-1 subtypes. *J. Acquir. Immune Defic. Syndr. 41*, 352–360.